11B.6 EFFECTS OF LAND-SEA ROUGHNESS CONTRAST ON TROPICAL CYCLONE WINDS

MARTIN L. M. WONG AND JOHNNY C. L. CHAN*
Laboratory for Atmospheric Research, Dept. of Physics and Mat. Sci., City University of Hong Kong

1. INTRODUCTION

Tropical cyclone (TC) landfall has been an important research problem due to the potentially huge destruction of lives and properties when the intense rainfall, severe winds and storm surge batter the coastal regions. Highly asymmetric structures of wind and rainfall usually accompany landfall. Previous idealized modeling and observational studies have documented the asymmetric convective activities during TC landfall (e.g. Chan and Liang 2003; Chan et al. 2004).

Wong and Chan (2006, hereafter WC06) found that the planetary boundary layer (PBL) convergence of the TC core could become strongly asymmetric even when the core TC circulation is completely away from the coast. They proposed the surface-induced asymmetric convergence as another factor that affects the asymmetric convective activities of the TC core. This paper focuses on understanding the asymmetric wind distribution of landfalling TCs. Idealized numerical experiments are performed with the Pennsylvania State University-National Center for Atmospheric Research MM5 model.

2. MODEL AND DESIGN OF EXPERIMENTS

a. MM5 model

Triply-nested square domains of 45, 15 and 5 km grid sizes have lengths of 6750, 2250 and 1200 km, respectively. There are 26 vertical layers. A constant Coriolis parameter at 15^{o}N is used. The surface fluxes and vertical diffusion are determined from a modified Mellor-Yamada level 2.5 PBL scheme. Except for the conceptual experiments, an explicit moisture prediction scheme and the Betts and Miller cumulus parameterization are also used.

b. Conceptual experiments

A vortex is spun-up on an *f* plane for a 24-h period after which it attains an intensity of ~ 976 hPa. The axisymmetric component of the mass and wind fields then form the initial conditions of the conceptual experiments, with the TC center placed at the center of the model domain. In all the experiments, a western portion of the surface is specified to be land of roughness length 0.5 m (sea roughness depends on wind strength), so that the TC is located at 50, 100, 150 km east (S50, S100, S150) and west (L50, L100, L150) of the north-south-oriented coastline, and right on the coastline (LS). Two more experiments with sea-only and land-only surfaces are also performed as control. The axisymmetric mass fields are held fixed during the 48-h simulation with the exclusion of moisture variables and latent heating. A quasi-steady state has been reached at the end of of each experiment. The hourly results for the second day (t = 24 to t = 48 h) are averaged and analyzed.

The use of time-invariant axisymmetric mass fields during the numerical integration requires justification, because we could simply analyze the results of the RD experiment of WC06 (inclusion of moisture effects and time-varying mass fields, see section 3b). There are 3 reasons. First, by fixing the mass fields, we expect to remove the effect of vertical shear which could force convective asymmetries. Second, for slow-moving TCs as in the RD case (~ 1 m s^{-1}), the asymmetry in the mass fields would be small. If a steering flow is present, we have to consider the associated asymmetry, but that would not highlight the effects due to the difference of surface roughness. Third, with the same mass fields for all the conceptual experiments, comparisons of the magnitudes of winds between the experiments could be made. In spite of these considerations, the results of the conceptual experiments and the RD experiment in WC06 are compared in section 3b.

For the conceptual experiments with the axisymmetric mass fields invariant in time and no moisture variables, only the momentum variables are allowed to change. After initial adjustments, a steady-state is reached. The equations for the radial wind u and tangential wind v are:

$$u\frac{\partial u}{\partial r}+\frac{v}{r}\frac{\partial u}{\partial \lambda}+w\frac{\partial u}{\partial z}=\frac{du}{dt}=\left(f+\frac{v}{r}\right)v-\frac{1}{\rho}\frac{\partial p}{\partial r}+D_u \quad (1)$$

$$u\frac{\partial v}{\partial r}+\frac{v}{r}\frac{\partial v}{\partial \lambda}+w\frac{\partial v}{\partial z}=\frac{dv}{dt}=-\left(f+\frac{v}{r}\right)u+D_v \quad (2)$$

where D_u and D_v are the diffusion terms that strongly depend on vertical diffusion and the surface fluxes of momentum, and all the other symbols carry their usual meaning. Willoughby (1990) argued that theoretically, axisymmetric supergradient flow could be realized by the inflow in the PBL, but observations do not support the systematic departure. On the other hand, the

* *Corresponding author address:* Johnny Chan, Department of Physics and Materials Science, City University of Hong Kong, Tat Chee Ave., Kowloon, Hong Kong, China. Email: Johnny.Chan@cityu.edu.hk

theoretical derivation and numerical simulation of Kepert (2001) and Kepert and Wang (2001) showed that a supergradient wind, primarily maintained by vertical advection, exists near the top of the PBL. In the following we will also discuss the wind distribution in terms of its deviation from the gradient wind.

3. RESULTS

a. Conceptual experiments

The lowest model level ($\sigma = 0.995$) has an elevation of 43 m above the surface and the maximum gradient wind speed is about 31 m s^{-1} at a radius of 50 km. The most obvious characteristic of the surface wind field is, as expected, the smaller wind speed over the land than the sea surface (Fig. 1). There are also some other important features that require explanations: First, the TC core winds are asymmetric even when the eye/eyewall region stays completely over the sea (Fig.1a) or land (Fig.1c). Before (after) landfall, the radial inflow is stronger (weaker) on the southwestern (northeastern) side where the flow is offshore (onshore). At the time of landfall, radial inflow is strong (weak) to the southeast (northwest) of the TC where the offshore (onshore) flow is in the southeast (northwest) quadrant (Fig. 1b). The maximum tangential wind occurs about 90 degrees downstream of the maximum radial inflow. Second, for pre-landfall and landfalling cases, the strongest inflow near the TC and the maximum tangential wind that occurs approximately 90 degrees downstream at a smaller radius are associated with the offshore flow. This is counter-intuitive as the offshore flow originates from the land surface of smaller wind speeds. Third, the maximum inflow and tangential winds for the LS case reach over 15 and 30 m s^{-1} respectively and are larger than those in the sea-only and land-only control experiments. Over the eastern core, the total wind speed is larger than the gradient wind speed in a considerable region (not shown).

To understand these results, it would be easier to think in terms of a 'thought experiment' where the sea-surface roughness is very small and the land-surface roughness is very large, and consider a single layer of air. Under such conditions, the radial flow for both control experiments would be nearly zero because the wind speed is very small for the land-only experiment and wind is in gradient balance for the sea-only experiment. Next we consider the simplified case corresponding to LS. For flow that has just moved offshore, the wind speed is small ($u, v \approx 0$) and diffusion terms have also become small ($D_u, D_v \approx 0$). According to (1) and (2) the air would be subjected to the pressure gradient force only and would undergo an inward acceleration. Radial inflow, which is absent in both control experiments, is produced. Moreover, although the kinetic energy of the flow that has just moved offshore is zero, it could become large due to the subsequent inflow and the work done by the pressure gradient force. The maximum total wind could be associated with the offshore flow if the air could move very close to the TC. In fact, a contraction of the left eyewall of hurricane Danny 1997 with associated maximum wind and rainfall was observed (Blackwell 2000). Moreover, the air that has just moved offshore is subjected to inward acceleration until the Coriolis and centrifugal forces balance the pressure gradient force in (1). However, the radial flow is still negative, which means that the tangential wind and total wind continue to increase according to (2). At this point, the total wind is already stronger than the (local) gradient wind due to the presence of the inflow. Gradually the radial acceleration becomes positive (or the tangential wind has become supergradient) and the radial inflow ceases at some small radius. This would explain why the tangential wind and total wind are larger then the gradient wind, and why the maximum radial inflow associated with the offshore flow for pre-landfall and landfalling cases could be stronger than both control experiments.

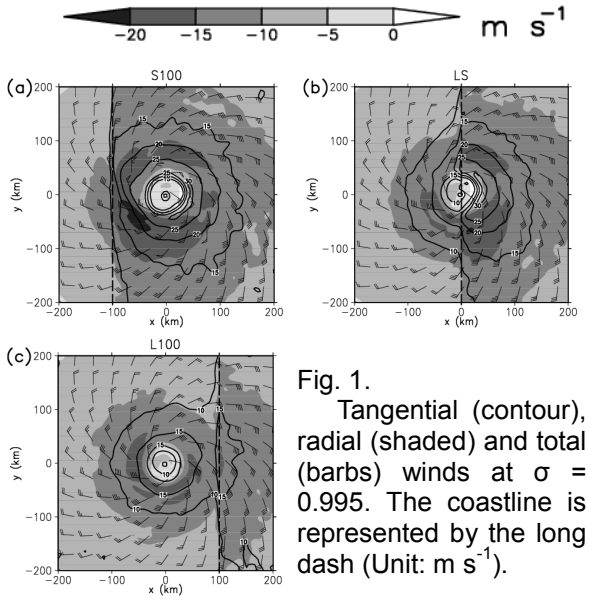

Fig. 1. Tangential (contour), radial (shaded) and total (barbs) winds at σ = 0.995. The coastline is represented by the long dash (Unit: m s^{-1}).

The above discussions remain valid in the experiments with reasonably large land-surface roughness and small sea-surface roughness, and a multi-layer atmosphere. In such conditions, the flow is not negligible over land. For the near-surface wind which is often of primary interest, D_u and D_v would not be zero for the air that has just moved offshore even if the sea surface is smooth (i.e. no surface fluxes), because air above the surface layer would import

momentum. The acceleration of the air due to a change of the roughness would be in the direction of the wind for the offshore flow and in the opposite direction of the wind for the onshore flow. Therefore, if the land surface is rough, the inflow angle is large and the offshore flow would undergo stronger inflow acceleration than a tangential acceleration. For the onshore flow, as the inflow angle over the sea is smaller, the air basically has a strong tangential deceleration, though the inflow deceleration is not negligible as in the landfalling and post-landfall cases.

The maximum tangential wind of 39 (42) m s^{-1} for the sea- (land-) only experiment is located at $\sigma = 0.94$ ($\sigma = 0.885$), or 522 (1024) m above mean-sea-level, and 50 (45) km from the TC center (not shown). It is about 24% (37%) supergradient, higher than the 10%-25% range found in Kepert and Wang (2001). The vertical advection in (1) is found to be the dominant contributor to the supergradient flow. For the experiments with a land-sea surface, the level of maximum wind over sea and land would differ. At $\sigma = 0.915$ for the LS case, maximum "supergradiency" (the excess of the Coriolis and centrifugal forces over the pressure gradient force) occurs to the south. The effects of tangential advection, radial advection, and vertical diffusion are found to be small so that the vertical advection explain most of the asymmetries (not shown).

An accompanying consequence of the asymmetric wind is the asymmetric vorticity and convergence. Except for the strongly positive relative vorticity in the TC core, the surface relative vorticity is characterized by a band of negative (positive) relative vorticity associated with the onshore (offshore) wind (not shown), in agreement with Tuleya and Kurihara (1978). We investigate the phase of the wavenumber-1 (WN1) convergence (both the radial and tangential components) of the surface horizontal wind ($-\nabla \cdot \mathbf{V}_h$) in 3 radial bands: (i) 0-50 km, (ii) 50-100 km and (iii) 100-500 km from the TC center. The phases for the various experiments show that except near the landfall position, strongest convergence occurs to the southwest or south for the 0-50 km band while it occurs to the west for the 50-100 km band (Fig. 2, large symbols). The phase for the LS case for the 0-50 km band shifted to the northeast quadrant because the area concerned includes the coastline. The differences using a stronger vortex are small (not shown). Decomposition of the convergences into tangential and radial components show that for the 0-50 km band, the asymmetry in convergence is strongly related to the radial wind except for the LS case where the tangential component is giving strong convergence to the north. For the 50-100 km band, both tangential and radial components contribute to the asymmetry of convergence while for the 100-500 km band, the tangential component dominates.

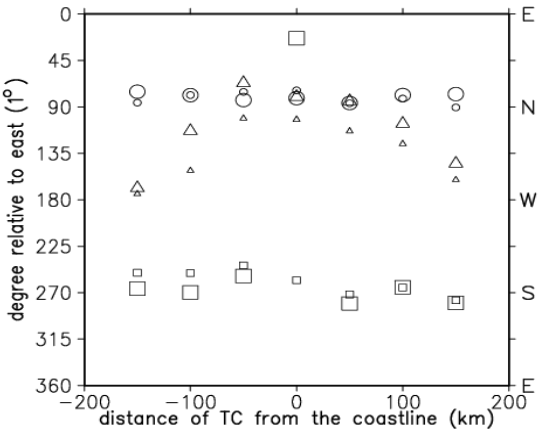

Fig. 2. Phase of the wavenumber-1 component of the surface (big symbols) and PBL (small symbols) convergences in the 0-50 km (squares), 50-100 km (triangles) and 100-500 km (circles) radial bands.

Wind gust prediction is also an essential element in a TC warning. Brasseur (2001) introduced a physical approach for gust estimation. For the LS case, the PBL height, defined here as the height at which the TKE drops below 0.6 m^2 s^{-2}, is higher over land and highest at the eyewall (not shown). The altitude for the maximum gust is also higher over land. However, the maximum gust is smaller over land because the wind is much smaller over land (Fig. 3). Overall, the gust factor is in a reasonable range.

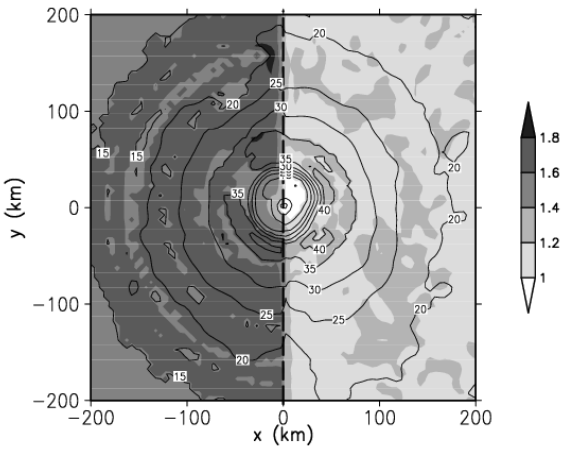

Fig. 3. Estimated maximum gust speed (contour) and gust factor (shaded) for the LS case. The TC center is at the origin and the vertical dashed line represents the coastline. (Unit: m s^{-1})

b. Full-physics experiment

In the RD experiment in WC06 the vortex initially 150 km east of the coast has drifted over land at the end of the 6-day simulation. Rainfall is larger over the south or southwest within 100 km from the TC surface center, but when the averaging distance is 300 km, rainfall is actually smallest to the south and strongest to the west, then gradually northwest as the TC approaches the coast and finally moved over land. These results agree fairly well with the phase of PBL convergence shown in Fig. 2 in two ways. First, the inner (0-50 km) and outer (100-500 km) PBL convergences are out of phase. Second, the phase of the PBL convergence in the middle (50-100 km) radial band rotates from northwest to north as the vortex 'approaches' the coast from the sea.

Supergradient surface tangential wind is also observed and is associated with the offshore flow. Just prior to landfall, the surface tangential wind is a maximum in the southeast while the maximum radial inflow occurs to the southwest (not shown). Moreover, the radii of maximum tangential and maximum radial winds are smaller (~ 20 km) just prior to landfall (not shown). Furthermore, the maximum tangential wind is supergradient when the TC is close to the coast (Fig. 4).

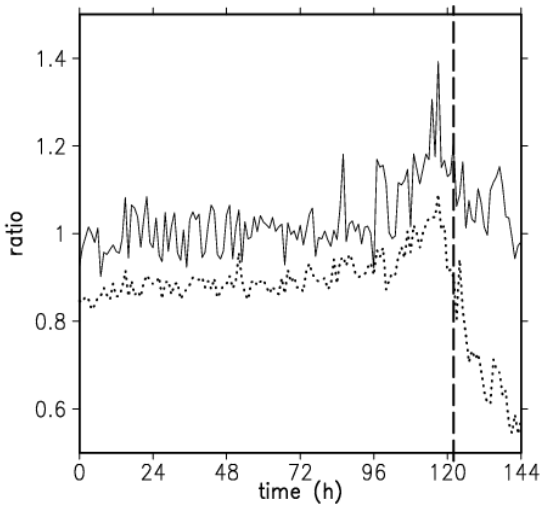

Fig. 4. Ratios of the maximum surface tangential wind to the local gradient wind (solid) and to the maximum surface gradient wind (dotted), for the RD experiment of WC06. The vertical dashed line marks the time of landfall at t = 122 h.

4. CONCLUDING REMARKS

The MM5 is used to simulate the tropical cyclone (TC) wind distribution near landfall under the idealized conditions of a dry atmosphere and time-invariant axisymmetric mass fields on an f plane. The winds are allowed to adjust towards a balance state under the influence of the different surface roughness between the land and sea, separated by a north-south-oriented coast. Consistent with theoretical reasoning, the results show that the surface-wind asymmetry near the TC core is related to the acceleration of the offshore (onshore) flow before (after) landfall. Estimation of wind gust has also been performed.

An obvious follow-up work would be to consider an asymmetry in the mass fields, especially those corresponding to a background flow or the β effect. Those effects would be more dominant and could improve further our understanding of the asymmetric TC structures forced by a land-sea surface. Moreover, we have only considered the surface momentum flux change under a roughly neutral condition. The validity of the results have to be verified against observations and more sophisticated simulations (includes radiation, soil predictions, etc).

Acknowledgments. This research is sponsored by the Research Grant Council of the Hong Kong Special Administrative Region, China Grant CityU 100203.

REFERENCES

Blackwell, K. G., 2000: The evolution of hurricane Danny (1997) at landfall: Doppler-observed eyewall replacement, vortex contraction/intensification, and low-level wind maxima. *Mon. Wea. Rev.,* **128,** 4002-4016.

Brasseur, O., 2001: Development and application of a physical approach to estimating wind gusts. *Mon. Wea. Rev.,* **129,** 5-25.

Chan, J. C. L., and X. Liang, 2003: Convective asymmetries associated with tropical cyclone landfall. Part I: *f*-plane simulations. *J. Atmos. Sci.,* **60,** 1560-1576.

Chan, J. C. L., K. S. Liu, S. E. Ching, and E. S. T. Lai, 2004: Asymmetric distribution of convection associated with tropical cyclones making landfall along the South China coast. *Mon. Wea. Rev.,* **132,** 2410-2420.

Kepert, J., 2001: The dynamics of boundary layer jets within the tropical cyclone core. Part I: Linear theory. *J. Atmos. Sci.,* **58,** 2469-2484.

Kepert, J., and Y. Wang, 2001: The dynamics of boundary layer jets within the tropical cyclone core. Part II: Nonlinear enhancement. *J. Atmos. Sci.,* **58,** 2485-2501.

Tuleya, R. E., and Y. Kurihara, 1978: A numerical simulation of the landfall of tropical cyclones. *J. Atmos. Sci.,* **35,** 242-257.

Willoughby, H. E., 1990: Gradient balance in tropical cyclones. *J. Atmos. Sci.,* **47,** 265-274.

Wong, M. L. M., and J. C. L. Chan, 2006: Tropical cyclone motion in response to land surface friction. *J. Atmos. Sci.,* accepted.